5-2017

Enzyme kinetics studies to guide mathematical modeling of microdialysis sampling to predict in situ biochemistry

Justin M. Klucher
University of Arkansas, Fayetteville

Enzyme kinetics studies to guide mathematical modeling of microdialysis sampling to predict *in situ* biochemistry

An honors thesis submitted in partial fulfillment

of the requirements for Honors Studies in

Chemistry and Biochemistry

By

Justin Klucher

2017

Chemistry / Biochemistry

J. William Fulbright College of Arts and Sciences

Acknowledgements

- My research mentor, Dr. Julie Stenken
- Kamel Alkhatib for helping me set up my experiments and guiding me through the process of microdialysis sampling
- The remainder of the Stenken Lab Group including Thad Vasicek, Alda Perez, Patrick Pysz, Randy Espinosa, Taylor Snider, and Kaleb Kougl
- The University of Arkansas Honors College for providing research and travel funding associated with this research
- NIH

Table of Contents

Abstract

Microdialysis is a diffusion-based sampling method that can be useful for monitoring various biological systems. Matrix metalloproteinases are a class of enzymes responsible for remodeling the extracellular matrix that, when dysregulated, are linked to various diseases. The delivery method of microdialysis is of particular interest as a sampling technique for enzymatic reactions. Microdialysis was performed *in vitro* using a model enzyme, porcine pancreatic elastase, because it is a useful substitute for matrix metalloproteinases. A colorimetric substrate for elastase, succinyl-ala-ala-ala-*p*-nitroanilide, and its product *p*-nitroaniline were measured using a UV-Vis spectrophotometer. Using an expanded Beer's Law equation, both analytes' concentrations were determined simultaneously from one dialysate sample using two of their overlapping absorbance wavelengths. The experiment aimed to test the effect flow rate, enzymatic solution concentration, and substrate concentration had upon the extraction efficiency of the procedure. Flow rate manipulations were consistent with literature, with higher flow rates yielding lower extraction efficiencies. Increasing the elastase concentration showed an increase in extraction efficiency of the substrate, whereas increasing the substrate concentration had no apparent effect on the extraction efficiency. Increasing either elastase or Succ-$(Ala)_3$-*p*-NA concentrations, however, yielded higher *p*-NA concentrations.

I. Introduction:

I. i. Overview:

Extracellular matrix (ECM) remodeling by proteases called matrix metalloproteinases (MMPs) is a critically important process that functions normally in embryogenesis or homeostasis, but potentially can become dysregulated leading to various self-destructive disease states. This class of 23 endopeptidases serves to remodel extracellular matrix proteins, such as collagen and elastase, plays a role in embryonic development, and studies have linked upregulated MMP concentrations to various disease states including arthritis, cancer and wound healing.[1, 2] Typically, many MMPs are activated simultaneously, thus monitoring the *in vivo* activity would be of clinical significance in recognizing when a patient may be at risk of dysregulated MMP activity.[5] Current methods to monitor the activity of MMPs include zymography, requiring extraction of whole tissue and a lengthy monitoring of both active and inactive forms of the enzymes[1], and immunochemical methods, though quantitative, cannot distinguish between active and pro-enzyme forms of the proteins.[4] Colorimetric assays are also used, however are limited by the fluorescent tags available and require LC MS procedures to distinguish. However, microdialysis sampling, used with judicious choices of substrates and an appropriate mathematical model, may allow for accurate monitoring of *in vivo* MMP activity in real time.

I. ii. Microdialysis Sampling

Microdialysis is a widely-used, minimally invasive, *in vivo* method to collect chemical components in tissue.[6] The process is performed using small probes with a 4-10 mm semi-permeable membrane tip of a specific molecular weight cutoff (MWCO), allowing size selective passage of molecules to diffuse in or out. A perfusion fluid, matching the sample solution's ionic

strength and chemical moiety, is loaded into a syringe and pumped through the inner membrane lumen at typical flow rates of 0.5-2.0 μL/min into a sample solution.[6] Analytes can also diffuse from the sample medium into the probe through a diffusion gradient as well. The target analytes, following diffusion into the probe, and any remaining perfusate travel through the outlet, as dialysate fluid, into a collection vial.[7-10] This process is summarized in Figure 1.

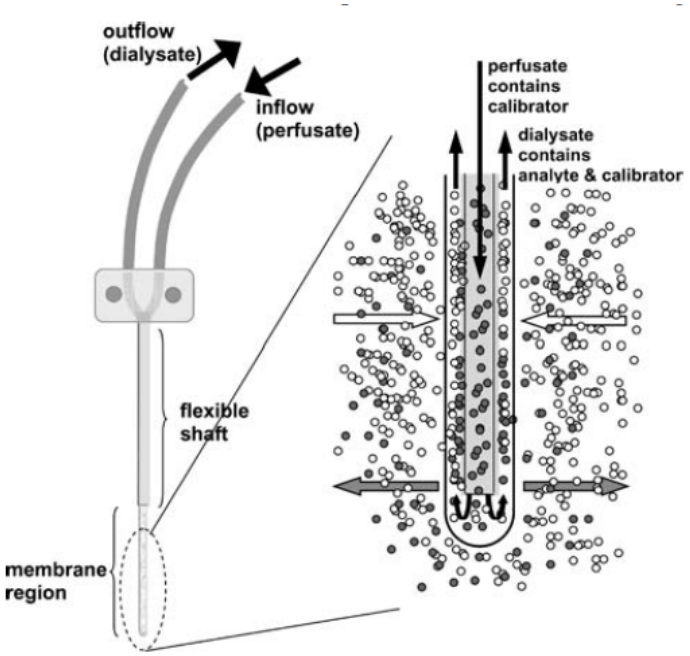

Figure 1: Diagram depicting diffusion-based movement of analyte using a microdialysis probe. Perfusate enters through the inlet and out of the inner tube where it can then interact with the semi-permeable membrane either diffusing into the solution or continuing into the dialysate. Analyte from the solution diffuses into the probe and is carried into the dialysate through the outlet tubing into a collection vial.[3]

Microdialysis as a sampling method holds several advantages to its usage. The size, usually 200-500 μm in diameter and 1-30 mm in length, allows minimally invasive *in vivo* sampling, with applications that began with studies in rat brain biochemistry to human studies of various organ systems.[6, 11] Another benefit comes from the semi-selectivity offered by the semi-permeable membrane. Depending on the probe's MWCO, a generic local sampling can be performed which could allow macromolecular sampling of proteins or selective sampling of low molecular weight compounds such as neurotransmitters or glucose. This provides a versatile applicability of microdialysis that cements its place as a useful biological sampling device.

Since microdialysis is often a function of variables like membrane length, membrane material, membrane MWCO, and diffusion coefficients, the extraction efficiency (EE) of microdialysis is usually displayed as a percentage, using Equation 1, to provide quantification of the probe's sampling efficiency.[4, 6] In this equation, C_{outlet} refers to the concentration of analyte collected as dialysate, C_{inlet} refers to the concentration of analyte present in the perfusate, and C_{sample} refers to the far-field concentration of analyte outside of the probe.

$$\mathrm{EE} = \frac{C_{outlet} - C_{inlet}}{C_{sample} - C_{inlet}} \times 100\% \quad (1)$$

By manipulating these concentrations, the extraction efficiency equation can be further modified into relative recovery (Equation 2), in which C_{inlet} is 0 and C_{sample} is assumed a finite amount, or delivery (Equation 3), in which C_{sample} is set to 0 and C_{inlet} is a finite amount. Recovery is useful for quantifying the effectiveness of microdialysis as a sampling tool for an unknown concentration of analyte in solution, whereas delivery (also known as loss) is beneficial in pharmacokinetic and activity assays of enzymes by introducing enzymatic substrate via the perfusate fluid into an enzymatic solution.

$$\text{Relative Recovery} = \mathrm{EE_{rec}} = \frac{C_{outlet}}{C_{sample}} \times 100\% \quad (2)$$

$$\text{Relative Delivery} = \mathrm{EE_{loss}} = \frac{C_{outlet} - C_{inlet}}{-C_{inlet}} \times 100\% \quad (3)$$

The delivery method of microdialysis is of interest because the coupling of size-selective permeability of the probe and proper analysis techniques of dialysate can allow local monitoring of *in situ* biological processes by instigating biochemical processes, such as an MMP reaction, by delivery of substrate and analysis of the recovered products with increased temporal resolution.

I. iii. Usage of an *in vitro* Enzymatic Model System

Sourcing MMPs is quite expensive, and as previously stated, they exist naturally as a mixture of MMP subtypes in a zymogen form until activated.[1, 4, 5] Because of this, it is difficult to perform controlled cost-efficient *in vivo* studies regarding MMPs. For this study, and many others preceding it,[1, 4, 5] porcine pancreatic elastase (PPE) is used as a useful model enzyme since it has the same substrate specificity as MMP-12, but at a fraction of the cost. Though all 23 MMPs are of clinical significance, MMP-12, or macrophage elastase, is one of interest due to it implication in emphysemas, abdominal aortic aneurysms, and atherosclerosis.[2] This MMP cleaves extracellular matrix proteins such as elastin, collagen, and fibrins normally, but can, when dysregulated, lead to the weakening of vital cardio-respiratory tissues due to this unregulated cleaving mechanism. Therefore despite PPE being used as preliminary model for one MMP, the MMP in question still has clinical relevance in developing a suitable sampling method.

PPE cleaves a colorimetric substrate, succinyl-trialanine-*p*-nitroanilide (Succ-$(Ala)_3$-*p*-NA), into the product *p*-nitroaniline (*p*-NA) and has been previously described for microdialysis studies by the Stenken group (Figure 2).[6] Due to the colorimetric metabolic product, UV-Vis spectrophotometry can be then used to quantify the recovered product and the EE of the delivered substrate as a method of quantifying the activity surrounding a microdialysis probe of a serine protease, elastase.

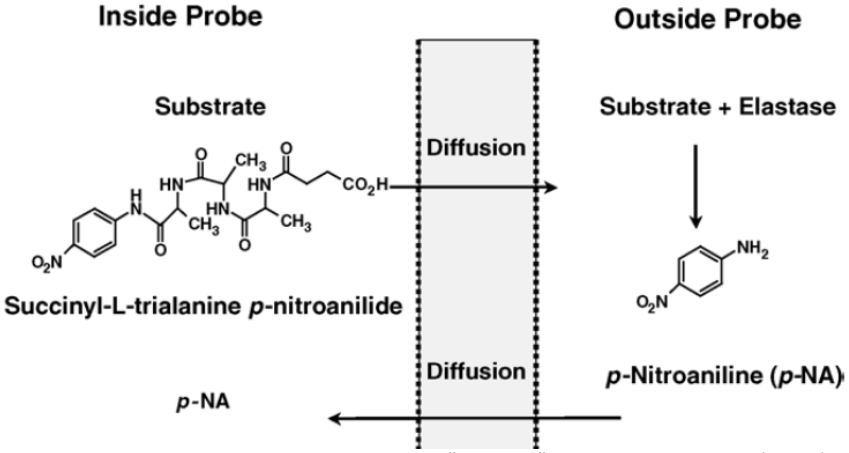

Figure 2: Diagram depicting a microdialysis probe in "Delivery" mode. The substrate (Succ-$(Ala)_3$-*p*-NA) is perfused through the probe so as to diffuse into a solution of elastase. The metabolic product (*p*-NA) is then diffused back into the probe as dialysate.[4]

I. iv. UV-Vis Spectrophotometry

Initially microdialysis was limited in its utility due to detection limitations requiring 50-100 μL samples to gain any appreciable readings of dialysate.[6] However, with current advances in analysis methods, this no longer acts as major impedance for microdialysis studies. A commonly used method to determine solution concentrations is spectrophotometry. Using Beer's Law (Equation 4), the absorbance of a chemical is directly proportional to the chemical's concentration, [X], its molar absorptivity, ε_x, and the path length, b (usually in values of 1 so as to be negligible).[12]

$$A = \varepsilon_x b[X] \tag{4}$$

Thus, Beer's Law allows the use of spectrophotometry to quantify dilute solutions such as the dialysate of a microdialysis sampling procedure. Thermo-Fischer's NanoDrop 2000c model is particularly useful in this regard as it can reliably measure the absorbance of aliquots as small as 1-2 μL in volume, a convenient amount since microdialysis collects at 0.5 to 2 μL/min rates normally. The low aliquot size for the NanoDrop eliminates one of the largest burdens with microdialysis, that being the time necessary to accumulate enough dialysate to make analytical measurements.

Substances have a maximum absorbance wavelength (λ_{max}) where the largest light absorbance occurs, however they can and will still absorb over a range of nearby wavelengths as well. In this experiment, a colorimetric substrate, Succ-$(Ala)_3$-*p*-NA, is cleaved into *p*-NA, however their maximum absorbance wavelengths overlap, and since they both will be present in the dialysate, the measurements at their respective maxima will not be sufficient to quantify their

concentrations as each chemical will contribute at each wavelength. This is because absorbance is an additive quantity, as expressed by equation 5.[12]

$$A' = \varepsilon'_x b[X] + \varepsilon'_y b[Y]$$

$$A'' = \varepsilon''_x b[X] + \varepsilon''_y b[Y] \quad (5)$$

In the above equations, A' refers to the total absorbance read by a spectrophotometer at one wavelength, a value made up of the Beer's law calculated absorbance for two separate chemicals, X and Y. Their combined absorbance makes up the absorbance measured by the spectrophotometer. A'' refers to the total absorbance at another wavelength. Each of these equations use different molar absorptivities specific to the chemical at that specific wavelength the spectrophotometer is measuring. Thus standards of each chemical can be produced to develop a calibration curve at both absorbance maximum wavelengths to determine their molar absorptivity. Since each quantity but the concentrations are known, a system of equations is possible using equation 6.[12]

$$[X] = \frac{\begin{vmatrix} A' & \varepsilon'_y b \\ A'' & \varepsilon''_y b \end{vmatrix}}{\begin{vmatrix} \varepsilon'_x b & \varepsilon'_y b \\ \varepsilon''_x b & \varepsilon''_y b \end{vmatrix}} \qquad [Y] = \frac{\begin{vmatrix} \varepsilon'_x b & A' \\ \varepsilon''_x b & A'' \end{vmatrix}}{\begin{vmatrix} \varepsilon'_x b & \varepsilon'_y b \\ \varepsilon''_x b & \varepsilon''_y b \end{vmatrix}} \quad (6)$$

The concentrations of *p*-NA and Succ-$(Ala)_3$-*p*-NA in the dialysate can thus be individually calculated in this method by solving the determinants present in the above equation after measuring the absorbance at both wavelength maxima.

II. Materials and Methods

II. i. Chemicals and Equipment

The enzyme, elastase from porcine pancreas (E1250), its substrate, N-succinyl-L-Ala-Ala-Ala -*p*-nitroanilide (S4760), and its colorimetric product, 4-nitroaniline (N2128) were purchased from Sigma Aldrich (St. Louis, MO). A 2 mM stock of Succ-$(Ala)_3$-*p*-NA in 10 mM PBS (pH=7.4) was produced from the Sigma solid; daily substrate solutions were diluted from this 2 mM solution for experimentation. Enzyme solutions were produced daily from the Sigma stock solution into a 10 mM PBS buffer (pH=7.4). For microdialysis, CMA/20 probes (MWCO 20 kDa) were purchased from Harvard Apparatus (Holliston, MA). The pumps (MD-1000), drivers (MD-1001), and 1 mL syringes (MDN-0100) used for microdialysis were purchased from BASi (West Lafayette, IN). Spectrophotometric analysis of the solutions was performed using a NanoDrop 2000c purchased from Thermo Fisher (Pittsburgh, PA).

II. ii. Formation of Calibration Curves for Substrate and Product

A 2 mM Succ-$(Ala)_3$-*p*-NA stock solution in 10 mM phosphate buffered saline at 7.4 pH was produced, from which a 1000 μM standard was pulled to determine the maximum absorbance wavelength of Succ-$(Ala)_3$-*p*-NA. Standards were also created for *p*-NA in this same manner. PBS was used to obtain the blank for the NanoDrop, and full UV-Vis absorbance scans were collected to determine the maximum absorbance wavelengths for Succ-$(Ala)_3$-*p*-NA and *p*-NA. From this reading, the largest absorbance peaks were selected for both chemicals, correlating to 315 nm for Succ-$(Ala)_3$-*p*-NA and 380 nm for *p*-NA. However, it was noted that the absorbance curves overlapped slightly for both chemicals at these wavelengths.

To produce calibration curves for the NanoDrop, the 1000 µM solutions were serially diluted to 500, 250, 125, 62.5, 31.25, and 15.625 µM solutions. These solutions were then analyzed within the NanoDrop in triplicate 2 µL aliquots at both 315 and 380 nm absorbance readings. This data was averaged and fitted with a linear trend in Excel to provide a calibration curve at each wavelength for both Succ-$(Ala)_3$-*p*-NA and *p*-NA. Beer's Law at a path length of 1 mm was used to determine the molar absorptivity of Succ-$(Ala)_3$-*p*-NA and *p*-NA at both 315 and 380 nm wavelengths using these calibration curves.

II. iii. Microdialysis Sampling

Microdialysis sampling experiments were performed several times while adjusting variables such as pump flow rate, enzyme concentration, and substrate concentration. The sampling technique used three CMA/20 probes (each having a 20 kDa MWCO) submerged in three 2 mL solutions of enzyme so as to fully cover the semi-permeable membrane of the probes. A pump delivered Succ-$(Ala)_3$-*p*-NA through the membrane inner lumen into the enzyme solution as perfusate allowing collection of *p*-NA and unreacted Succ-$(Ala)_3$-*p*-NA as dialysate. The pump perfused Succ-$(Ala)_3$-*p*-NA, loaded into three syringes, through the attached probes for a set amount of time so as to collect approximately 10 µL of dialysate. The probes were flushed with HPLC grade water for 15 minutes before and after any procedure at 3 µL/min.

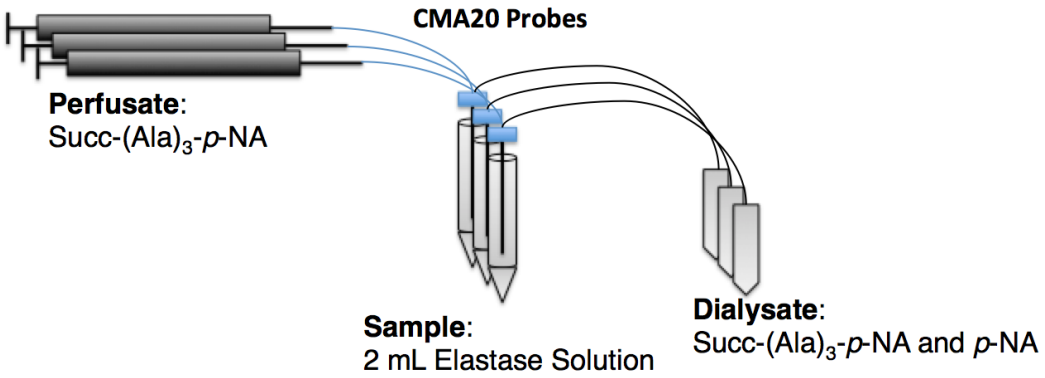

Figure 3: Microdialysis setup used in these experiments. Three syringes, loaded with Succ-$(Ala)_3$-*p*-NA solutions, connect to three separate probes submerged in elastase solutions. The outlets empty into separate microcentrifuge vials.

The first experiment tested the fluid delivery of HPLC water from the pump and syringes using FEP tubing into collection vials to ensure calibration of the equipment. The pump was set to 3 µL/min perfusion, and fluid was collected for 5 minutes. Using gravimetric analysis, the volume of the delivered fluid was determined and compared to the pump's flow rate setting. This was repeated again with the probes attached to the syringes in place of the FEP tubing. Results were consistent with the pump's flow rate settings (data not reported).

Next, delivery of 1000 µM Succ-$(Ala)_3$-*p*-NA into 2 mL PBS buffer solutions were performed at 1.5, 1.0, and 0.8 µL/min flow rates at 7, 10, and 12.5 min intervals, respectively. For this experiment nine buffer solutions were made so that fresh solutions were used for each flow rate for each probe. The probes were allowed to equilibrate at the desired flow rate for 15 minutes prior to dialysate collection so as to flush the probes of previous analyte concentrations. Dialysate was collected into empty 1.5 mL microcentrifuge vials for each probe at each flow rate.

The remaining experiments adjusted either enzyme concentration or substrate concentration using the same procedure as outlined above for the flow rate manipulations with minor variations. In the enzyme manipulation experiment, 1000 µM Succ-$(Ala)_3$-*p*-NA was perfused at 1.5 µL/min into three sets of three 2 mL elastase solutions at 2.0, 1.0, and 0.5 unit/mL elastase concentrations, made by serial dilution from the Sigma stock, for 7 minutes. The substrate manipulation experiment perfused 1000, 500, and 250 µM Succ-$(Ala)_3$-*p*-NA solutions perfused at 1.5 µL/min into three sets of three 2 mL elastase solutions at 1.0 unit/mL elastase concentration. In each of these experiments the same equilibration method was used. Both experiments were performed at room (21° C) and physiological (37° C) temperature.

II. iv. Dialysate Concentration Determination Using NanoDrop Spectrophotometry

The dialysate collected from each of the above outlined procedures held enough fluid for triplicate 2 μL aliquot readings with some excess if necessary. Each aliquot was measured at 315 and 380 nm absorbance. These readings were averaged between the three probes and used for the following calculations. A system of Beer's Law equations produced from the calibration curves was used to determine the concentration of Succ-$(Ala)_3$-*p*-NA and *p*-NA present in the dialysate. The concentration of the Succ-$(Ala)_3$-*p*-NA concentrations loaded into each syringe were also collected and measured using the NanoDrop in the same manner. The perfusate and dialysate concentrations were then compared to determine EE_{loss} of substrate.

III. Results and Discussion

III. i. Absorbance Spectra and Calibration Curves for Analytes

Prior to further experimentation it was necessary to determine the absorbance characteristics of the two analytes being measured in these experiments, Succ-$(Ala)_3$-*p*-NA and *p*-NA. From the prepared 1000 μM samples of either analyte, absorbance spectra were measured using the NanoDrop spectrophotometer for both Succ-$(Ala)_3$-*p*-NA and *p*-NA. These spectra are both displayed overlaid in Figure 4. As can be seen in the diagram, both analytes' maximum absorbance wavelengths partially overlap requiring the expanded Beer's Law equation discussed earlier (Equation 5). Using the maximum wavelengths, 315 nm for Succ-$(Ala)_3$-*p*-NA and 380 nm for *p*-NA, together provides a larger signal for measurement for both analytes, and also offers a method to determine the concentrations of two analytes simultaneously from one dialysate sample.

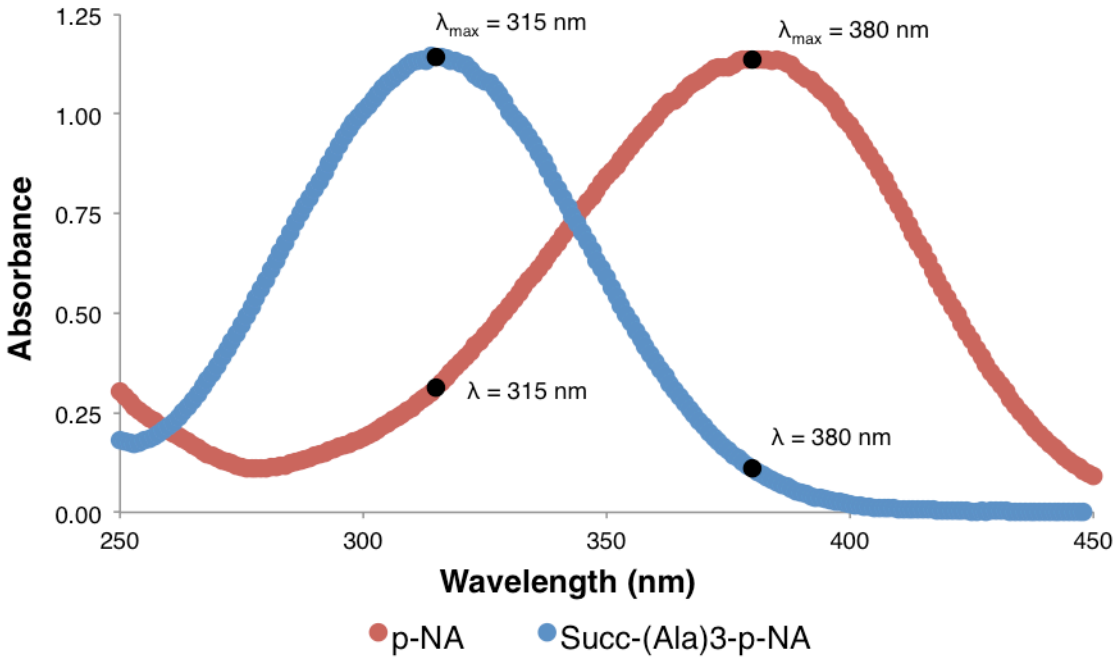

Figure 4: Absorbance spectra measured for 1000 µM Succ-$(Ala)_3$-*p*-NA and 1000 µM *p*-NA. The maxima are labeled as well as the corresponding measurement on the non-dominant spectra showing the overlap of the absorbance measurements due to the combination of unreacted Succ-$(Ala)_3$-*p*-NA substrate and p-NA product that would be present in microdialysis dialysate.

After determination of the absorbance spectra, the 1000 µM samples of Succ-$(Ala)_3$-*p*-NA and *p*-NA were serially diluted to form a series of standards from which calibration curves were constructed using the absorbance measurements at both 315 and 380 nm for both analytes. These curves are expressed as Figures 5 and 6 for Succ-$(Ala)_3$-*p*-NA and *p*-NA respectively. The slopes of these curves represent the molar absorptivity, ε, times the path length as shown by Beer's Law. Since the path length is 1 mm for the NanoDrop 2000c, the slopes of the curves were used as the molar absorptivities corresponding to 315 and 380 nm for both Succ-$(Ala)_3$-*p*-NA and *p*-NA that were used for future experiments. These values are displayed in Table 1 and match relatively consistently to previously reported values from the Stenken Lab.[13]

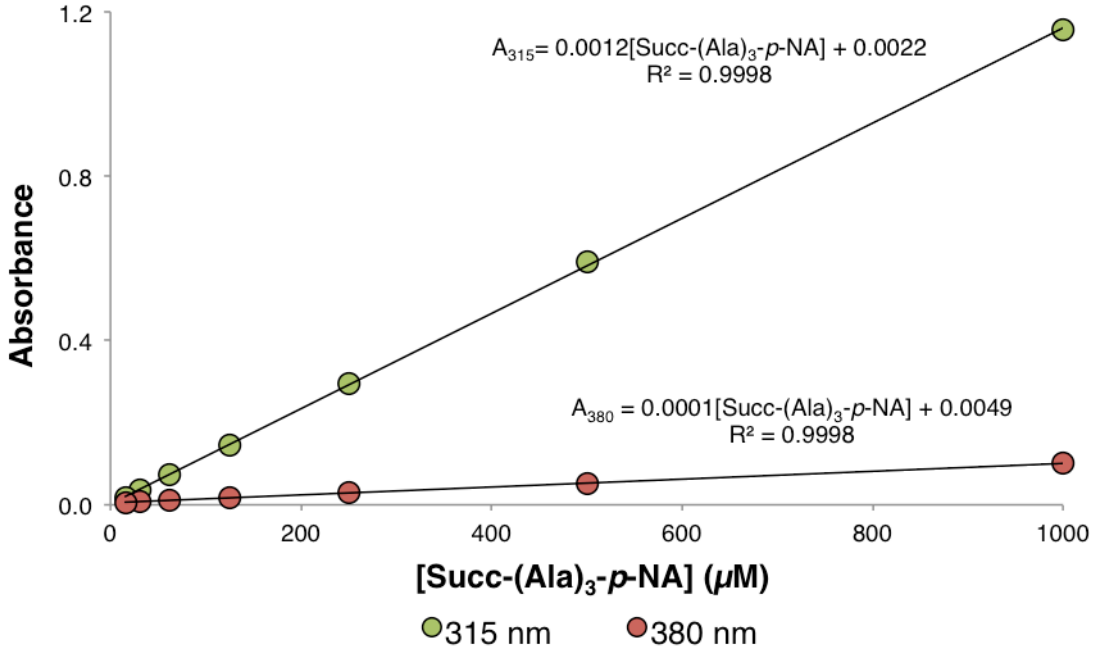

Figure 5: Calibration curve formed from 1000, 500, 250, 125, 62.5, 31.25, and 15.625 µM standards of Succ-$(Ala)_3$-*p*-NA in 10 mM PBS (pH=7.4). Data points represented as averaged absorbance measurements at 315 and 380 nm using a NanoDrop 2000c (n=3).

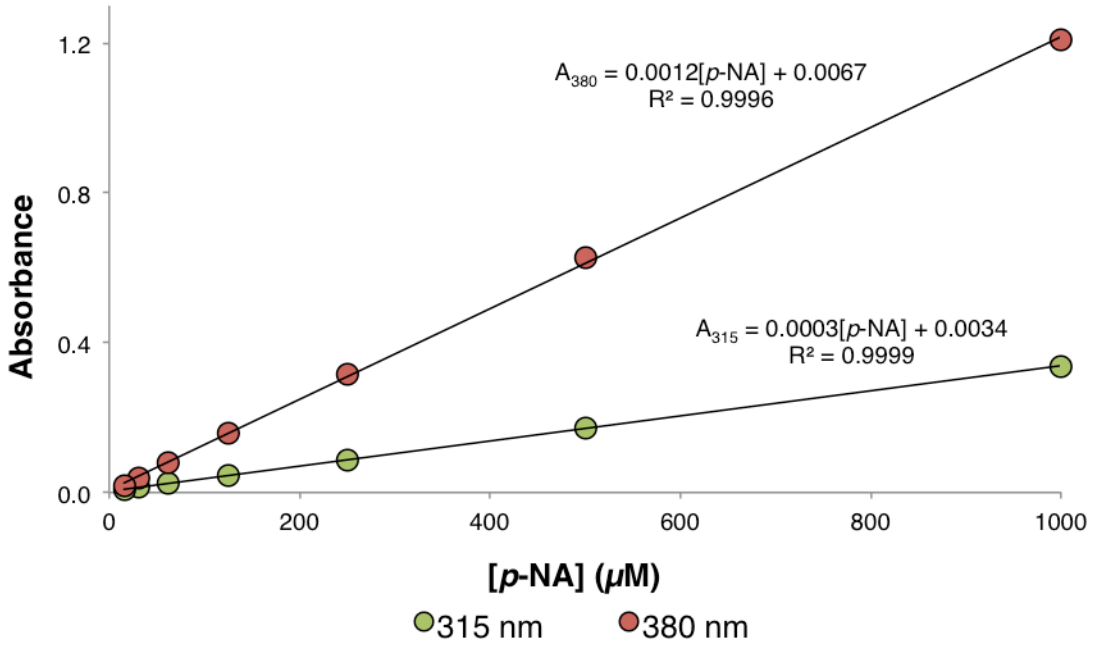

Figure 6: Calibration curve formed from 1000, 500, 250, 125, 62.5, 31.25, and 15.625 µM standards of *p*-NA in 10 mM PBS (pH=7.4). Data points represented as mean absorbance measurements at 315 and 380 nm using a NanoDrop 2000c (n=3).

Table 1: Molar absorptivities for Succ-$(Ala)_3$-*p*-NA and *p*-NA at both 315 and 380 nm derived from calibration curves to be used in Beer's Law calculations to determine dialysate analyte concentrations of either molecule. The molar absorptivities are labeled in the form $\varepsilon_{X,Y}$ Where X specifies the analyte, S for Succ-$(Ala)_3$-*p*-NA and P for *p*-NA, and Y specifies the wavelength the absorptivity corresponds.

Succ-$(Ala)_3$-*p*-NA		*p*-NA	
$\varepsilon_{S,315}$ (μM^{-1} mm^{-1})	0.0012	$\varepsilon_{P,315}$ (μM^{-1} mm^{-1})	0.0003
$\varepsilon_{S,380}$ (μM^{-1} mm^{-1})	0.0001	$\varepsilon_{P,380}$ (μM^{-1} mm^{-1})	0.0012

As can be seen from the calibration curves, there is a slight, but apparent, overlap in absorbance contributions from either analyte at the respective wavelengths. It is because of this that the four molar absorptivities displayed in Table 1 will need to be used in conjunction with Beer's Law and the matrix equation shown before (Equation 6) to determine the combined dialysate concentrations of each analyte.

III. ii. Microdialysis Flow Rate Manipulation Results

After the calibration curves were developed, microdialysis experiments were performed to test the effect on EE_{loss} (Delivery) and product formation under various conditions. The first experiment tested the effect flow rate had upon EE_{loss} by eluting 1000 μM Succ-$(Ala)_3$-*p*-NA through three probes to be delivered into triplicate 2 mL sample of 10 mM PBS buffer without enzyme present. The dialysate absorbance measurements were then used to determine the Succ-$(Ala)_3$-*p*-NA concentration remaining in dialysate. Since no enzyme was present, no *p*-NA was present in the dialysate and a simplified Beer's Law equation using only the 315 nm molar absorptivity was used to calculate the concentration. The results of this experiment are presented in Figure 7. The results of this experiment show a decrease in extraction efficiency for microdialysis as flow rate increases. This trend is well established in the literature[4, 6] occurring due to a lower residency time for analytes to successfully diffuse through the semi-permeable membrane. Since the flow rates used in this experiment are relatively close together in

magnitude the decrease appears linear. However, were the flow rate manipulations increased upwards of 5 µL/min a more exponential decrease would likely occur. This experiment was only performed at room temperature (21° C), however had it been a higher temperature the extraction efficiency would likely be systematically raised at each flow rate due to temperature having a proportionate role in determination of diffusion coefficients. Data was not collected to test this hypothesis for this experiment, however.

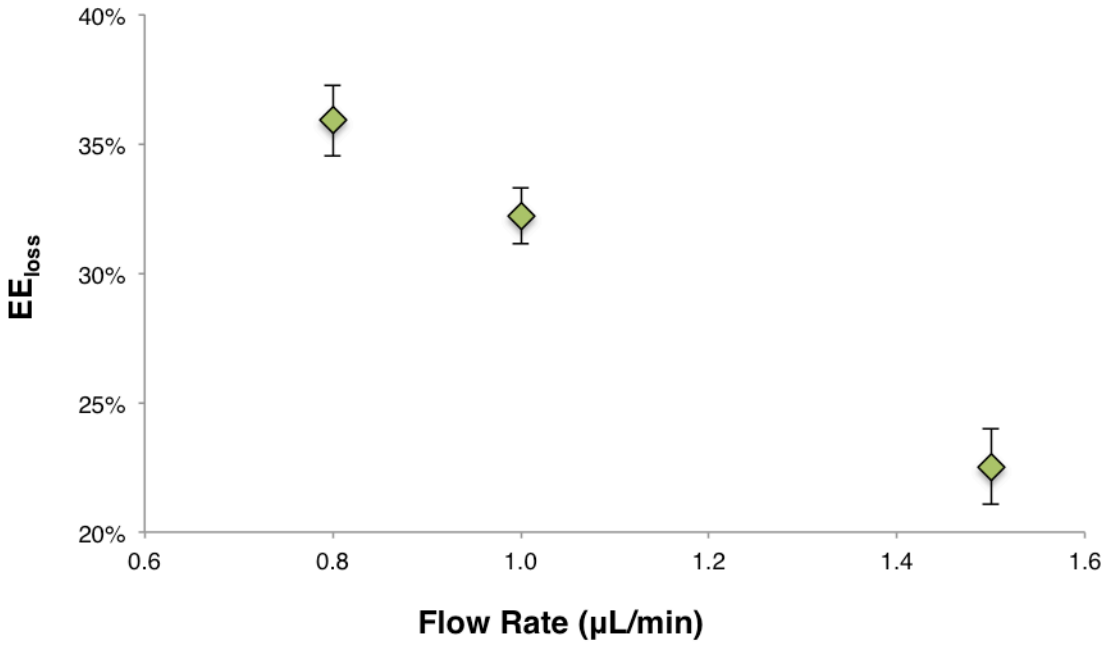

Figure 7: Flow rate vs EE_{loss} of a microdialysis-based delivery of 1000 µM Succ-$(Ala)_3$-*p*-NA eluted at 0.8, 1.0, and 1.5 µL/min flow rates for 12.5, 10, and 7 min respectively into a 2 mL solution of 10 mM PBS (pH=7.4) at 21° C . There was no Elastase enzyme present in the samples. Data represented as mean ± SD.

Though the 1.5 µL/min yielded the lowest EE_{loss} of the three flow rates tested, it was used for all subsequent experiments since it yielded quantifiable concentrations of Succ-$(Ala)_3$-*p*-NA and would only need to elute for approximately 7 minutes to provide enough dialysate for triplicate measurements using the NanoDrop spectrophotometer.

III. iii. Microdialysis Enzyme Concentration Manipulation Results

While EE_{loss} can be directly manipulated through judicious choice of flow rate, this experiment aimed to note the effect that manipulating the concentration of the enzymatic solution itself had on EE_{loss} for the microdialysis delivery. To do this, the concentration of elastase enzyme present in the solution was adjusted through serial dilution to produce triplicate 0.5, 1.0, and 2.0 unit/mL elastase solutions in 2 mL centrifuge vials. Following the elution of 1000 µM Succ-$(Ala)_3$-*p*-NA into these solutions for 15 minutes of equilibration and 7 minutes of collection, the dialysate was analyzed using the NanoDrop spectrophotometer at 315 and 380 nm. The results of this experiment are displayed in Table 2 as well as Figures 8 and 9.

Table 2: Results of eluting 1000 µM Succ-$(Ala)_3$-*p*-NA into increasing concentrations of elastase solution. Data for 21° C and 37° C experiments are shown. Elution allowed to equilibrate for 15 min and collect for 7 min at 1.5 µL/min. Data represented as mean ± SD (n=3)

[Elastase] (unit/mL)	[Succ-$(Ala)_3$-*p*-NA] Lost (µM)	[*p*-NA] Recovered (µM)	[*p*-NA]/[Succ-$(Ala)_3$-*p*-NA] (%)	EE_{loss} (%)
0.5	344.00 ± 13.01	85.92 ± 5.20	25.34 ± 1.91	35.45 ± 1.37
1.0	402.14 ± 9.87	109.64 ± 4.85	27.26 ± 1.34	41.44 ± 1.07
2.0	415.97 ± 13.65	133.41 ± 4.91	32.09 ± 1.66	42.87 ± 1.45
0.5*	372.82 ± 11.57	101.86 ± 2.80	27.32 ± 1.13	39.34 ± 1.29
1.0*	432. 52 ± 11.29	130.47 ± 4.30	30.16 ± 1.27	45.64 ± 1.28
2.0 *	525.56 ± 11.55	209.00 ± 6.86	39.77 ± 1.57	55.46 ± 1.35

* Represents the solution at 37° C

The results of this experiment show that the concentration of the enzyme present in the sampled solution has an apparent effect on the EE_{loss} of the microdialysis technique. There is an observable positive trend correlated with the extraction efficiency as the sample's elastase concentration increases. What this implies is a stronger delivery of Succ-$(Ala)_3$-*p*-NA into the solution from the microdialysis probe while also producing a stronger *p*-NA yield due to an increase in delivered Succ-$(Ala)_3$-*p*-NA to react. The product recovery increase is likely further explained due to an increased amount of available elastase active sites to facilitate the reaction.

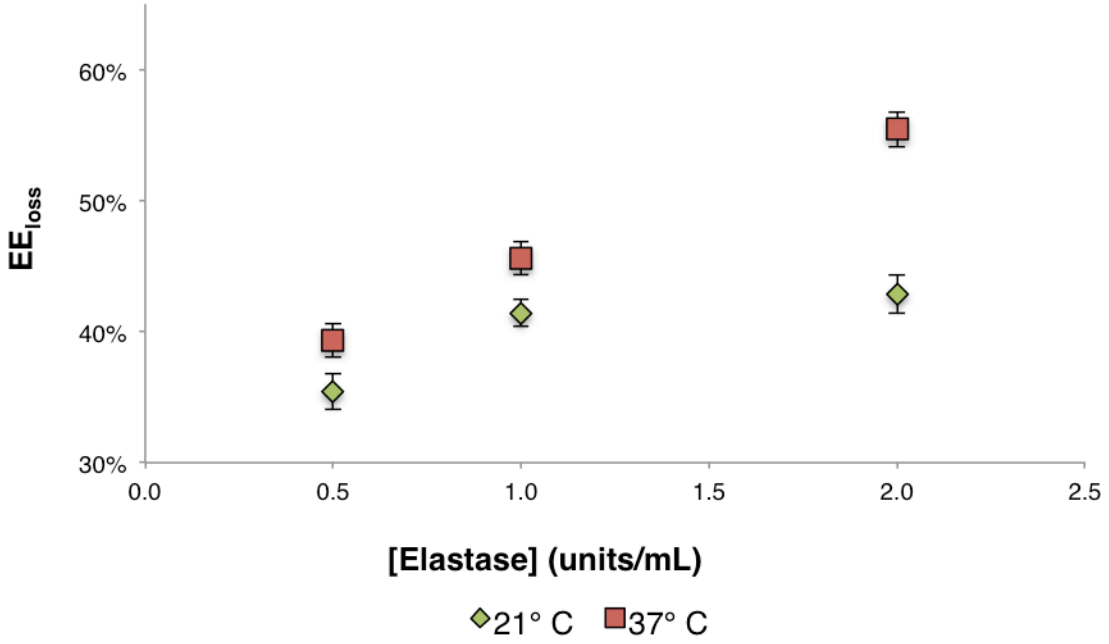

Figure 8: Elastase sample concentration vs. EE_{loss} of microdialysis delivery of 1000 µM Succ-$(Ala)_3$-*p*-NA into triplicate 2 mL elastase solutions (pH=7.4) at 0.5, 1.0, and 2.0 units/mL. Solutions allowed to equilibrate for 15 mins prior to a 7 min collection at 1.5 µL/min flow rate. Data represented as mean ± SD (n=3).

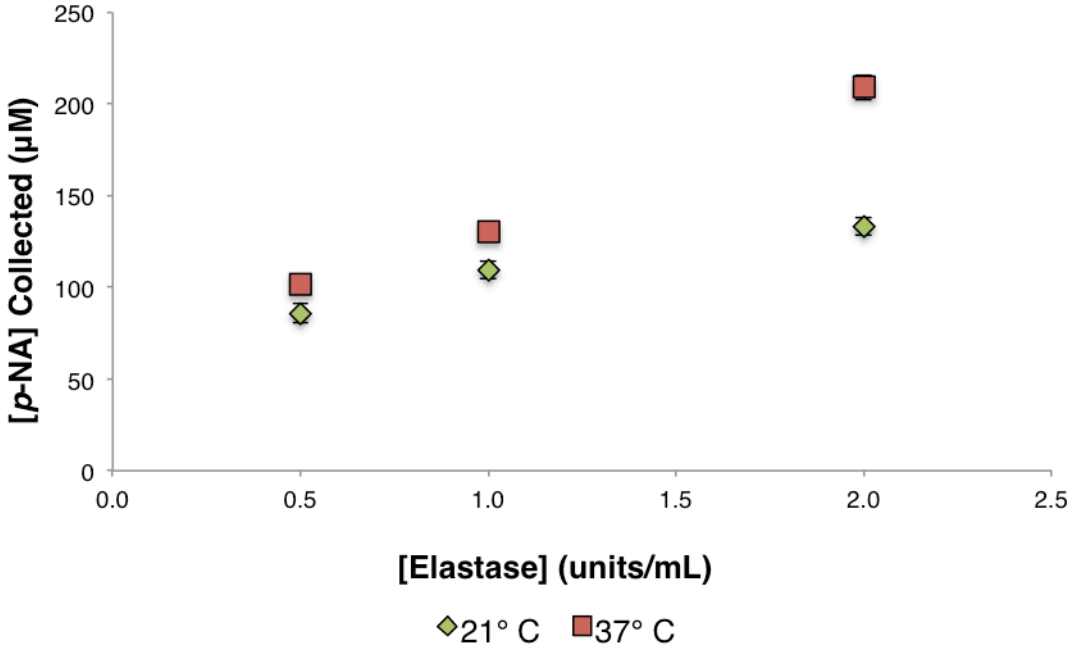

Figure 9: Elastase concentration vs. product (*p*-NA) collected in dialysate following delivery of 1000 µM Succ-$(Ala)_3$-*p*-NA into triplicate 2 mL elastase solutions (pH=7.4) at 0.5, 1.0, and 2.0 units/mL. Solutions allowed to equilibrate for 15 minutes prior to a 7 min collection at 1.5 µL/min flow rate. Data represented as mean ± SD (n=3).

This increased EE_{loss} is likely explained by concentration gradients. In the event of an increased enzyme concentration, more active sites remain available to collect the substrate, Succ-$(Ala)_3$-*p*-NA. This reduces the apparent concentration of substrate in the solution as compared to a lower concentrated enzymatic solution since more substrate is bound as an enzyme-substrate complex. Thus this further facilitates the diffusion of Succ-$(Ala)_3$-*p*-NA into the solution since the concentration of the Succ-$(Ala)_3$-*p*-NA in the solution is reduced faster in the same amount of time due to the presence of more enzyme. This in turn, on the other hand, increases the apparent concentration of *p*-NA in solution following the reaction since more substrate can react in the same amount of time, further facilitating the diffusion of *p*-NA into the probe for recovery down its now increased concentration gradient. This trend is more apparent in Table 2 by comparing the ratio of recovered *p*-NA to the lost Succ-$(Ala)_3$-*p*-NA. As the concentration of the elastase sample increased so did this ratio. This implies that the rate at which the *p*-NA is recovered is slightly higher than the rate at which the Succ-$(Ala)_3$-*p*-NA is being delivered, otherwise the ratio would decrease as the elastase concentration increased. These experiments were performed at room temperature (21° C) and physiological (37° C), and at the higher temperature the data appears to show the same trend, however systematically shifted upward likely due to the increased activity of the elastase enzyme at its preferred temperature condition. The results of this experiment could prove to be useful information since a noticeable trend can be seen to be associated with the EE_{loss} of a microdialysis delivery into solutions of increased enzymatic concentrations. Normally EE_{loss} is varied by flow rate manipulations by researchers, but the data appears to suggest the properties of the sample itself can also impact the delivery.

III. iv. Microdialysis Substrate Concentration Manipulation Results

The next experiment tested the effect manipulation of the Succ-$(Ala)_3$-*p*-NA concentration in the perfusate had upon EE_{loss} and *p*-NA recovery. In this experiment, serially diluted concentrations of 250, 500, and 1000 µM Succ-$(Ala)_3$-*p*-NA were delivered into three sets of triplicate 2 mL 1.0 unit/mL solutions of elastase. As before, each concentration of Succ-$(Ala)_3$-*p*-NA was eluted for 15 minutes of equilibration and 7 minutes of collection, the dialysate of which was analyzed at 315 and 380 nm absorbance wavelengths to determine the concentration of *p*-NA and unreacted Succ-$(Ala)_3$-p-NA. The results of these experiments are displayed in Table 3 and Figures 10 and 11.

Table 3: Results of eluting 250, 500, and 1000 µM Succ-$(Ala)_3$-*p*-NA into 1.0 unit/mL elastase solutions. (Note: the concentrations listed in the table reflect the concentration of syringe perfusate measured through UV-Vis spectrophotometry following each elution) Data for 21° C and 37° C experiments are shown. Elution allowed to equilibrate for 15 min and collect for 7 min at 1.5 µL/min. Data represented as mean ± SD (n=3)

[Succ-$(Ala)_3$-*p*-NA] (µM)	[Succ-$(Ala)_3$-*p*-NA] Lost (µM)	[*p*-NA] Recovered (µM)	[*p*-NA]/[Succ-$(Ala)_3$-*p*-NA] (%)	EE_{loss} (%)
240.15 ± 2.11	92.23 ± 5.04	36.88 ± 2.95	39.99 ± 3.87	38.40 ± 2.12
489.04 ± 2.21	187.23 ± 6.17	71.72 ± 15.35	38.31 ± 8.30	38.28 ± 1.27
954.01 ± 6.53	373.90 ± 9.93	111.99 ± 6.40	29.95 ± 1.89	39.19 ± 1.07
242.29 ± 3.02*	136.06 ± 6.17	45.06 ± 4.67	33.12 ± 3.75	56.16 ± 2.64
489.51 ± 0.97*	264.58 ± 5.88	88.39 ± 4.12	33.41 ± 1.72	54.05 ± 1.32
941.00 ± 8.52*	586.92 ± 8.91	217.35 ± 4.47	37.03 ± 0.95	62.37 ± 1.10

* Represents the solution at 37° C

The results of this experiment show a slightly different trend than when the elastase concentration was manipulated. From the data presented in Figure 10, it appears that increasing the substrate concentration does not have a significant effect on the EE_{loss} of the microdialysis delivery method. At each concentration the EE_{loss} remains relatively constant at approximately 38% for room temperature (21° C) and approximately 56% for physiological (37° C). However, it does seem that the physiological 1000 µM EE_{loss} breaks this trend slightly. This may be due to difficulty observed in the lab at maintaining the sand bath used for the experiment at 37° C.

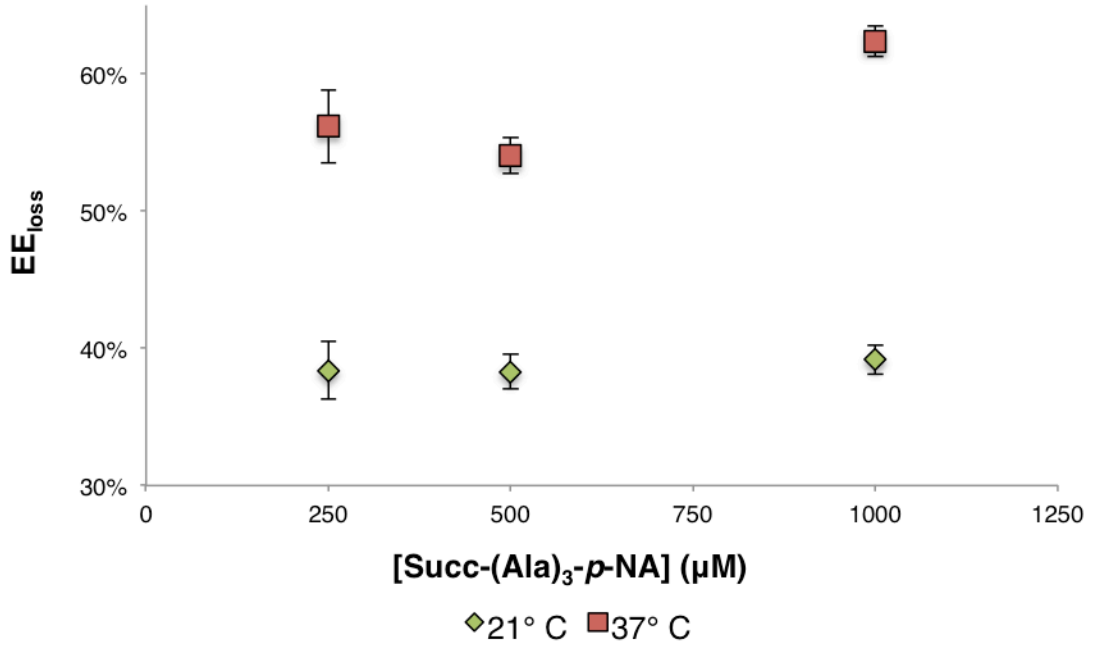

Figure 10: Succ-$(Ala)_3$-*p*-NA concentration vs. EE_{loss} of microdialysis delivery of various concentrations of Succ-$(Ala)_3$-*p*-NA into triplicate 2 mL elastase solutions (pH=7.4) at 1.0 unit/mL. Solutions allowed to equilibrate for 15 mins prior to a 7 min collection at 1.5 µL/min flow rate. Data represented as mean ± SD (n=3).

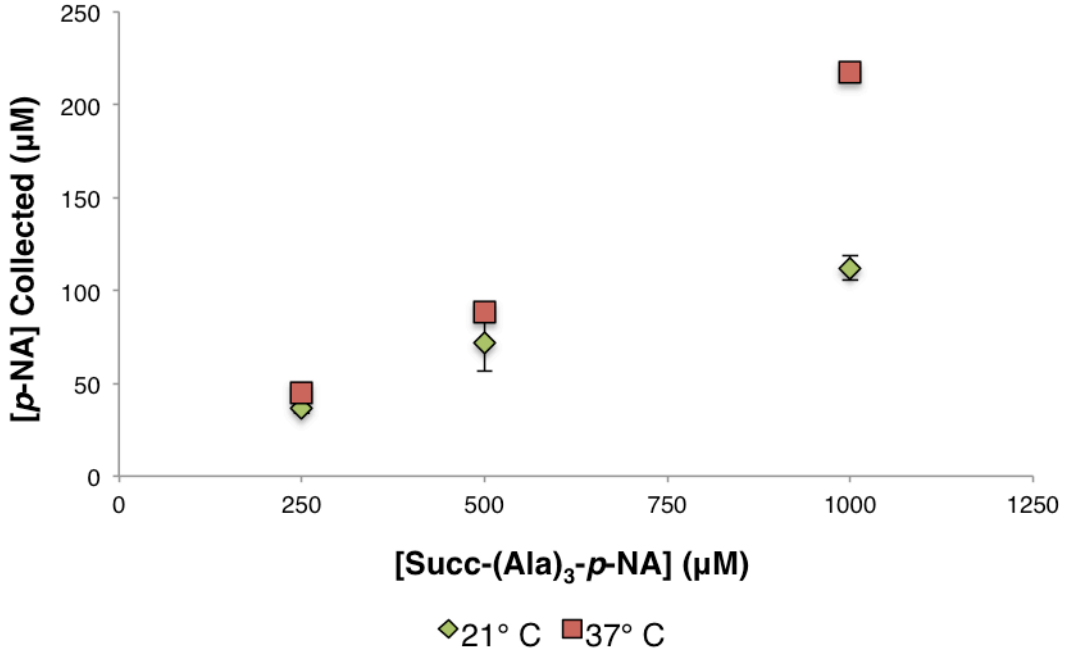

Figure 11: Succ-$(Ala)_3$-*p*-NA concentration vs. product (*p*-NA) collected in dialysate following delivery of various concentrations of Succ-$(Ala)_3$-*p*-NA into triplicate 2 mL elastase solutions (pH=7.4) at 1.0 unit/mL. Solutions allowed to equilibrate for 15 minutes prior to a 7 min collection at 1.5 µL/min flow rate. Data represented as mean ± SD (n=3).

Regardless, manipulating the substrate appears to have little to no effect on the EE_{loss} of the delivery. This is likely occurring because the enzyme concentration is not changing. It remains at 1.0 unit/mL and thus becomes saturated with Succ-$(Ala)_3$-*p*-NA faster reducing the enhanced diffusion that was suspected in the previous experiment. Without this increased diffusion, the delivery thus becomes flow rate dependent likely resulting in the constancy of the EE_{loss}. The increased temperature does appear to raise the EE_{loss} systematically by a much higher degree than in the previous experiment however. This could also be due to the inconsistent temperature readings observed in the lab, but it may also be due to a combined effect the temperature has upon the process. The increased temperature will raise the activity of the elastase allowing it to facilitate the biochemical reaction faster in the same amount of time, encouraging the trend seen in the previous experiment, but also the increased temperature will proportionally increase the diffusion coefficients according to Fick's Law. However, this doesn't explain why the same magnitude of increase was not experienced in the previous experiment. Further replications of this experiment are likely necessary to gain a better understanding of this phenomenon. Similarly to the previous experiment, the *p*-NA concentration increases with Succ-$(Ala)_3$-*p*-NA concentration since higher amounts of substrate are able to diffuse into the solution if the perfusate is at a higher concentration. The steep slope experienced at the physiological temperature suggests that this reaction is substrate limited and has not yet approached Michaelis-Menten equilibrium. However, the lower temperature appears to have begun to plateau suggesting an enzyme limitation. While an increase in the EE_{loss} was not observed, a much larger magnitude of recovered product was achieved between substrate concentrations. This could be useful in artificially boosting the analyte signal for measuring the activity of an enzyme in

question by encouraging a stronger product output by increasing the substrate eluted to facilitate the reaction.

IV. Conclusion

Microdialysis could prove to be both a viable and useful method for instigating biochemical reactions *in vitro*. The experiments reinforced literature observations linking increased flow rates to decreased extraction efficiencies, further establishing the need to use low flow rates to achieve the highest resolution of results. The results of the experiments further suggested that the extraction efficiency of the microdialysis delivery method is linked to the activity of the enzyme in the solution, increasing the effectiveness of the delivery itself and the output of product. This conclusion appears further supported by the absence of this trend when adjusting the Succ-$(Ala)_3$-*p*-NA concentrations instead. Some problems arose when trying to raise the temperature of the solutions to physiological ranges due to observed uneven heating that could have potentially skewed several of the results in this paper. To correct this, further replicative experiments should be performed to determine if these were out of character results. This could potentially be translated towards monitoring *in vivo* systems as a means of sampling enzymatic processes. However, much more work will be necessary to account for increased variables of a biological system as well as a means to model this behavior neatly for intuitive use.

Works Cited

1. Wang, Y.; Zagorevski, D. V.; Stenken, J. A., In situ and multisubstrate detection of elastase enzymatic activity external to microdialysis sampling probes using LC-ESI-MS. *Anal Chem* **2008,** *80* (6), 2050-7.

2. Bordenave, T.; Helle, M.; Beau, F.; Georgiadis, D.; Tepshi, L.; Bernes, M.; Ye, Y.; Levenez, L.; Poquet, E.; Nozach, H.; Razavian, M.; Toczek, J.; Stura, E. A.; Dive, V.; Sadeghi, M. M.; Devel, L., Synthesis and in Vitro and in Vivo Evaluation of MMP-12 Selective Optical Probes. *Bioconjug Chem* **2016**.

3. Chaurasia, C.; Müller, M.; Bashaw, E.; Benfeldt, E.; Bolinder, J.; Bullock, R.; Bungay, P.; Delange, E.; Derendorf, H.; Elmquist, W.; Nordstrom, C.; Rollema, H.; Sawchuk, R.; Cheung, B.; Shah, V.; Stahle, L.; Ungerstedt, U.; Welty, D.; Yeo, H., AAPS-FDA Workshop White Paper: Microdialysis Principles, Application and Regulatory Perspectives. *Pharmaceutical Research* **2006,** *24* (5), 1014-1025.

4. Steuerwald, A. J.; Villeneuve, J. D.; Sun, L.; Stenken, J. A., In vitro characterization of an in situ microdialysis sampling assay for elastase activity detection. *J Pharm Biomed Anal* **2006,** *40* (5), 1041-7.

5. Wang, Y.; Zagorevski, D. V.; Lennartz, M. R.; Loegering, D. J.; Stenken, J. A., Detection of in vivo matrix metalloproteinase activity using microdialysis sampling and liquid chromatography/mass spectrometry. *Anal Chem* **2009,** *81* (24), 9961-71.

6. Stenken, J. A., Microdialysis Sampling. In *Encyclopedia of Medical Devices and Instrumentation*, Webster, J. G., Ed. Wiley-Interscience: Hoboken, N.J., **2006**; pp 400-420.

7. Westerink, B. H. C.; Cremers, T. I. F. H., *Handbook of Microdialysis Sampling: Methods, Applications, and Clinical Aspects*. Academic Press: Amsterdam, **2007**.

8. Müller, M., *Microdialysis in Drug Development*. AAPS Springer: New York, **2013**; Vol. 4.

9. Timofeev, I.; Carpenter, K. L. H.; Nortje, J.; Al-Rawi, P. G.; O'Connell, M. T.; Czosnyka, M.; Smielewski, P.; Pickard, J. D.; Menon, D. K.; Kirkpatrick, P. J.; Gupta, A. K.; Hutchinson, P. J., Cerebral extracellular chemistry and outcome following traumatic brain injury: a microdialysis study of 223 patients. *Brain* **2011,** *134* (Pt 2), 484-94.

10. Shannon, R. J.; Carpenter, K. L. H.; Guilfoyle, M. R.; Helmy, A.; Hutchinson, P. J., Cerebral microdialysis in clinical studies of drugs: pharmacokinetic applications. *J. Pharmacokinet. Pharmacodyn.* **2013,** *40* (3), 343-358.

11. Stenken, J. A.; Ståhle, L.; Lunte, C. E.; Southard, M. Z., Monitoring in situ liver metabolism in rats using microdialysis. Comparison of microdialysis mass-transport model predictions to experimental metabolite generation data. *J Pharm Sci* **1998,** *87* (3), 311-20.

12. Harris, D., *Quantitative Chemical Analysis*. 8th ed.; Macmillan: **2010**.

13. Baioni, N. E., Development toward fluorescence imaging of microdialysis sampling diffusion profiles. Chemistry and Biochemistry Undergraduate Honors Theses. **2015**.